The Origin of Chaos in the Outer Solar System

N. Murray[1] and M. Holman[2]

Classical analytic theories of the solar system indicate that it is stable, but numerical integrations suggest that it is chaotic. This disagreement is resolved by a new analytic theory. The theory shows that the chaos among the jovian planets results from the overlap of the components of a mean motion resonance among Jupiter, Saturn, and Uranus, and provides rough estimates of the Lyapunov time (10^7 years) and the dynamical lifetime of Uranus (10^{18} years). The jovian planets must have entered the resonance after all the gas and most of the planetesimals in the protoplanetary disk were removed.

The predictability of planetary motions was largely responsible for the acceptance of Newton's theory of gravitation. Despite this, Newton doubted the long-term stability of the solar system. Laplace noted that the ratios μ of planetary masses M to solar mass $M_\odot$ are small ($\mu \approx 10^{-3}$ to 10^{-9}), as are the planet's orbital eccentricities $e \approx 10^{-2}$ and inclinations $i \approx 10^{-2}$ (in radians). Neglecting terms proportional to second or higher powers of these quantities, Laplace showed that the motions of the planets were stable (*1*). In this century, Arnold showed that for μ, e, and i of order 10^{-43}, most planetary systems, in the sense of measure theory, are stable and undergo quasiperiodic but bounded variations in semimajor axis (a), e, and i for each planet (*2*). However, the values of the small quantities in our solar system are much larger than 10^{-43}, so the applicability of Arnold's theory is uncertain. Studies over the last decade have been dominated by brute force numerical integration. Sussman and Wisdom (*3*) and Laskar (*4*) performed numerical integrations of the planet's orbits and found positive Lyapunov exponents, indicating that they are chaotic. Sussman and Wisdom also showed that integrations of the jovian planets Jupiter, Saturn, Uranus, and Neptune are by themselves chaotic. In neither case are the variations in a, e, and i quasiperiodic, nor is it clear that they are bounded. Are the numerical results incorrect, or are the classical calculations simply inapplicable?

We show analytically that the results of Laplace and Arnold do not apply to our solar system. The chaos seen in integrations of the outer planets arises from the overlap of the components of a three-body mean motion resonance among Jupiter, Saturn, and Uranus, with a minor role played by a similar resonance among Saturn, Uranus, and Neptune. We test the theory using a suite of numerical integrations. The widths $\Delta a/a$ of the individual resonances are of order 3×10^{-6}, so that small changes in the initial conditions of the planets can lead to regular motion. This explains the puzzling dependence of Lyapunov time with integration step size seen in the outer planet integrations of Sussman and Wisdom (*3*). However, the uncertainties in the initial conditions, and those introduced by our numerical model, are comfortably smaller than the width of the individual resonances, so our solar system is almost certainly chaotic. The resonance is extremely weak and hence easily disrupted. Torques exerted on the planets by the protoplanetary gas disk and by planetesimals were orders of magnitude larger than the resonant torques, so most of the planetesimals and all the gas must have been cleared from the outer solar system before the planets entered the resonance.

Analytic Theory

Orbital dynamics. Planets in the solar system follow nearly Keplerian orbits (*5*). The orbit of each planet can be thought of as consisting of three nonlinear oscillators, corresponding to the three spatial directions. The Kepler problem is unusual in that all three oscillations have the same frequency. The orbital elements were chosen to take advantage of this degeneracy. The angle l varies on the orbital time scale, whereas the angle ω describing radial motion and the angle Ω describing vertical motion are fixed. In the actual solar system ω and Ω are time-dependent, with frequencies denoted by g_j and s_j, respectively. These frequencies are proportional to the mass ratios μ, and are consequently much smaller than the mean motion $n = dl/dt$, the time rate of change of the mean anomaly. Although our model contains only the jovian planets, we label g_j and s_j with j = 5, 6, 7, and 8, corresponding to the radial order of the planets in the solar system. The mean motions n (in units of cycles per day) and the modal frequencies of the jovian planets were determined by numerical integration of the equations of motion (Table 1). Each planet's elements vary with all the frequencies s and g. In the case of Jupiter,

$$e_J \sin \omega_J \approx e_{55} \sin(g_5 t + \xi_5) + e_{56} \sin(g_6 t + \xi_6) + \ldots \qquad (1)$$

where $e_{55} \approx 0.044$, $e_{56} \approx 0.016$, and ξ_5 and ξ_6 are constants.

Resonances and chaos. A resonance occurs when two or more oscillators are coupled in such a way that a linear combination of their angles $\sigma \equiv \Sigma_i p_i \theta_i$ undergoes a bounded oscillation, in which case σ is said to librate. In the sum defining σ, i denotes the ith oscillator and the p_i's are (possibly negative) integers. When the oscillators are not resonant, all possible combinations of θ_i's increase or decrease indefinitely, in which case σ is said to rotate. The physical significance of a resonance is that energy is exchanged between the oscillators over a libration period, which is large compared to the oscillation period of any of the oscillators. This prolonged exchange can lead to large changes in the motion of the system. The orbit that divides regions of phase space where σ librates from those where σ rotates is called the separatrix.

The other bit of dynamics needed to understand our result is the notion of resonance overlap. Chaos in Hamiltonian systems, of which the motions of the planets are an example, arises when the separatrix of one resonance is perturbed by another resonance. The extent of the chaos depends on the stochasticity parameter K, which is a function of the separatrix width divided by the distance between resonances. If K is small, there is little chaos, but for $K > 1$ the region in the immediate vicinity of the resonances is primarily chaotic (*6*). An orbit that, at different times, both librates and rotates must cross the separatrix, and is therefore chaotic. Another signature of chaos is that two initially nearby chaotic orbits diverge exponentially with

Table 1. Orbital frequencies of the giant planets. Data are from our numerical integrations.

Planet/mode	$n/2\pi$ (days^{-1})	g (days^{-1})	s (days^{-1})
5	2.308×10^{-4}	8.967×10^{-9}	0.0
6	9.294×10^{-5}	5.965×10^{-8}	-5.564×10^{-8}
7	3.259×10^{-5}	6.520×10^{-9}	-6.328×10^{-9}
8	1.662×10^{-5}	1.420×10^{-9}	-1.460×10^{-9}

[1]Canadian Institute for Theoretical Astrophysics, University of Toronto, 60 St. George Street, Toronto, Ontario M5S 3H8, Canada. [2]Harvard-Smithsonian Center for Astrophysics, 60 Garden Street, Cambridge, MA 02138, USA.

time; in our numerical work we use both diagnostics.

Two-body mean motion resonances. Two planets are said to be in a mean motion resonance when $p_1 d\lambda_1/dt \approx p_2 d\lambda_2/dt$. In that case, conjunctions between the planets occur at nearly fixed locations in space. The designation "mean motion" is a little misleading, because if $p_1 \neq p_2$ there is no coupling between the (λ,a) motion of two planets that does not involve a third degree of freedom, either the radial (ω,e) or vertical (Ω,i) motion of at least one of the planets (*7*).

There are no two-body mean motion resonances among the planets. However, there is a near–mean motion resonance between Jupiter and Saturn; Jupiter makes five circuits around the sun in about the same time that Saturn orbits twice. Saturn affects the orbit of Jupiter through its gravity, described by the potential

$$\phi = -\left(GM_S/|\mathbf{r}_J - \mathbf{r}_S|\right) \qquad (2)$$

where M_S is the mass of Saturn, $\mathbf{r}_J$ and $\mathbf{r}_S$ are the position vectors of Jupiter and Saturn, and G is the gravitational constant. To see the resonance mathematically, we expand $\mathbf{r}_J$ and $\mathbf{r}_S$ in terms of the orbital elements of the two planets, keeping only the lowest order terms:

$$\begin{aligned}\phi = & -(GM_S/a_S)\Sigma_{k,q,p,r}\phi^{(2,5)}_{k,q,p,r}(a_S/a_J) \\ & \times e_S^k e_J^q i_S^p i_J^r \cos(2\lambda_J - 5\lambda_S \\ & + k\omega_S + q\omega_J + p\Omega_S + r\Omega_J)\end{aligned} \qquad (3)$$

The amplitudes $\phi_{k,q,p,r}$ can be found in classic references (*8*). Symmetry considerations show that the integers in the argument of the cosine must sum to zero, $2 - 5 + k + q + p + r = 0$, and that $p + r$ must be even. This result shows explicitly that the gravitational coupling between two bodies on Keplerian orbits always involves either (ω,e) or (Ω,i), so that at least three oscillators are affected. To lowest order in the eccentricities and inclinations, the integers k, q, p, and r are non-negative and must sum to 3. The strength of the coupling is proportional to e^3 or ei^2, so this resonance is said to be of third order. Hence there are 10 frequencies associated with the resonance, four involving only perihelion precession rates, such as

$$2\dot{\lambda}_J - 5\dot{\lambda}_S + 2\dot{\omega}_J + \dot{\omega}_S \qquad (4)$$

and six involving the precession rates of the nodal lines, including

$$2\dot{\lambda}_J - 5\dot{\lambda}_S + \dot{\omega}_J + \dot{\Omega}_J + \dot{\Omega}_S \qquad (5)$$

The dot over the angles in these expressions denotes a time derivative. Each of the 10 members of Eq. 3 is referred to as a resonant term or, sometimes, as a resonance. The reason for this misuse of terminology is that, although none of the frequencies associated with these terms in our solar system vanish, they are much smaller than the mean motions of Jupiter and Saturn. As a result, the resonant terms have a strong effect on the orbits of the two planets.

Eighteenth-century astronomers, unaware of the significance of these long-period terms, noted a discrepancy between the predicted and observed longitudes of Jupiter and Saturn. This discrepancy, known as the great inequality (*9*), was finally explained by Laplace. He noted that the resonant terms given by Eq. 3 force a periodic displacement of 21 arc min in Jupiter's longitude and 49 arc min in Saturn's, showing that the predictions of the law of gravitation agreed with observations of the two planets.

The largest effect of Saturn's gravity on e_J is the secular variation described by Eq. 1. However, the most relevant component of Saturn's gravity for chaotic motion is described by Eq. 3. This component forces much smaller variations in $e_J \sin \omega_J$, given by

$$\begin{aligned} e_J^{2,5} \sin\omega_J \approx & \{\mu_S/[2 - 5(n_S/n_J)]\} \\ & \times (a_J/a_S)\Sigma_{p>0}\phi^{(2,5)}_{k,p,q,r}\, e_S^k e_J^{p-1} i_J^q i_S^r \\ & \times \sin[2\lambda_J - 5\lambda_S + k\omega_S + (p-1)\omega_J \\ & + q\Omega_J + r\Omega_S]\end{aligned} \qquad (6)$$

The largest variation in $e_J^{2,5}$, corresponding to $k = 2, p - 1 = q = r = 0$, and $\phi_{2,1,0,0} \approx 9.6$, has an amplitude of $\sim 3.5 \times 10^{-4}$. Our numerical integrations yield 3.7×10^{-4}, consistent within the errors introduced by keeping only the highest order term in e. This variation in e_J plays a central role in producing chaos among the outer planets.

There are other two-body near–mean motion resonances in the solar system. Of particular relevance here is the $7\lambda_U - \lambda_J$ near-resonance between Jupiter and Uranus. The potential experienced by Uranus is

$$\begin{aligned}\phi = & -(GM_J/a_U)\Sigma_{k,q,p,r}\phi^{(7,1)}_{k,q,p,r} \\ & \times e_J^k e_U^q i_J^p i_U^r \cos[\lambda_J - 7\lambda_U + k\omega_J \\ & + q\omega_U + p\Omega_J + r\Omega_U]\end{aligned} \qquad (7)$$

To lowest order (sixth) in e and i, there are 44 terms. The coefficients $\phi^{(7,1)}_{k,q,p,r}$ range from $\sim 10^{-3}$ to ~ 10. By itself this resonance has little effect on the dynamics of the solar system.

Three-body mean motion resonances. Now consider the fact that $e_J \sin \omega_J$ varies; substituting Eq. 6 into Eq. 7, we find the potential experienced by Uranus due to the non-Keplerian orbit of Jupiter:

$$\begin{aligned}\phi \approx & -(GM_J/a_U)\mu_S\varepsilon_{JS}^{-1}\alpha_{JS} \\ & \times \Sigma_{p=0}^{5}(6-p)\phi^{(7,1)}_{6-p,p,0,0}\phi^{(5,2)}_{2,1,0,0}\, e_J^{5-p} e_U^p e_S^2 \\ & \times \sin[3\lambda_J - 5\lambda_S - 7\lambda_U + 7\omega_J \\ & + p(\omega_U - \omega_J) + 2\omega_S]\end{aligned} \qquad (8)$$

where $\alpha_{JS} = a_J/a_S \approx 0.55$ and $\varepsilon_{JS} = |2 - 5(n_S/n_J)| \approx 1.3 \times 10^{-2}$. For simplicity we have ignored terms involving the inclinations and kept only terms proportional to e_S^2. This three-body mean motion resonance is second order in the masses of the planets (both μ_J and μ_S appear) and seventh order in e.

Using the frequencies in Table 2 and accounting for terms involving i, we find a mixed e-i resonance at $a_U \approx 19.21796$ AU associated with the argument

$$3\lambda_J - 5\lambda_S - 7\lambda_U + 7g_6t + 2s_7t \qquad (9)$$

We find a cluster of eccentricity resonances centered at $a_U \approx 19.2163$ AU with argument

$$3\lambda_J - 5\lambda_S - 7\lambda_U + (2-q)g_5t + 7g_6t + qg_7t \qquad (10)$$

where $0 \leq q \leq 2$, and at $a_U \approx 19.2193$ AU with argument

$$3\lambda_J - 5\lambda_S - 7\lambda_U + (3-q)g_5t + 6g_6t + qg_7t \qquad (11)$$

where $0 \leq q \leq 3$. At the present epoch, the JPL ephemeris DE200 has $a_U \approx 19.21895$ AU.

For simplicity we have described only one type of term in the potential experienced by Uranus: that due to the influence of Jupiter as it moves in the potential of the sun and Saturn, as reflected in $e_J \sin \omega_J$. There are similar contributions to the potential due to variations in Jupiter's other orbital elements. Moreover, there are weaker resonances due to the gravity of Saturn, moving on an orbit perturbed by Jupiter, and acting on Uranus. Finally, there are much smaller terms due to the direct perturbations of Uranus by Saturn and Jupiter moving on their unperturbed Keplerian orbits.

We also find three-body resonances with arguments containing

$$3\lambda_S - 5\lambda_U - 7\lambda_N + 7g_6t + (2-q)s_7t + qs_8t \qquad (12)$$

at 19.2187 AU $\lesssim a_U \lesssim$ 19.2195 AU. The strength of the resonance is smaller than that of the resonance involving Jupiter by the ratio $(\mu_N/\mu_J)(\varepsilon_{JS}/\varepsilon_{SU}) \approx 3 \times 10^{-3}$.

Table 2. Masses, in units of the solar mass $M_\odot$, and the current semimajor axes a, eccentricities e, and inclinations i of the orbits of the giant planets. Data are taken from JPL ephemeris DE200.

Planet	$\mu \equiv M/M_\odot$	a (AU)	e	i (radians)
Jupiter	9.548×10^{-4}	5.207	0.04749	0.02277
Saturn	2.859×10^{-4}	9.553	0.05274	0.04338
Uranus	4.355×10^{-5}	19.219	0.04641	0.01348
Neptune	5.178×10^{-5}	30.111	0.00820	0.03089

Overlapping resonances. The overlap of the individual resonances produces chaos among the outer planets. The width of a typical component resonance is

$$\Delta a/a_{\rm U} = 8[(6-p)\phi^{(7,1)}_{6-p,p,0,0} \times \phi^{(2,5)}_{2,1,0,0}(\alpha/3\varepsilon_{\rm JS})\mu_{\rm J}\mu_{\rm S}e_{\rm J}^{5-p}e_{\rm U}^{p}e_{\rm S}^{2}]^{1/2} \approx 2\times10^{-6} \quad (13)$$

or $\Delta a \approx 8 \times 10^{-5}$ AU. We must substitute powers of either e_{55} or e_{56} for $e_{\rm J}^{5-p}$, depending on the resonant argument. This resonance width is comparable to the radius of Uranus. The libration period is

$$T_0 = T_{\rm U}\Big/[147(6-p)\phi^{(7,1)}_{6-p,p,0,0} \times \phi^{(2,5)}_{2,1,0,0}(\alpha/\varepsilon_{\rm JS})\mu_{\rm J}\mu_{\rm S}e_{\rm J}^{5-p}e_{\rm U}^{p}e_{\rm S}^{2}]^{1/2} \approx 10^7 \text{ years} \quad (14)$$

The precession frequencies g_5 and g_7 determine the distance between the component resonances; we find

$$\delta a/a_{\rm U} \approx (4\pi/21)[(g_5-g_7)/n_{\rm U}] \approx 7\times10^{-6} \quad (15)$$

The stochasticity parameter is

$$K \equiv [\pi(\Delta a/\delta a)]^2 \quad (16)$$

Using Eqs. 13 and 15 in Eq. 16, we see that $K \gtrsim 1$, so the motion is marginally chaotic. Then the Lyapunov time (the inverse of the Lyapunov exponent) is given by $T_{\rm L} \lesssim T_0$ (*10*).

The chaotic nature of the system ensures that the angles in the perturbing potential (Eq. 8) experienced by Uranus are essentially random variables. These chaotic perturbations force Uranus's e to undergo a random walk, exploring all values between 0 and $e_{\rm cross} \approx 0.5$; for $e > e_{\rm cross}$ Uranus will suffer close encounters with Saturn, and may be ejected from the solar system. The time for this to occur is of order

$$T_{\rm cross} \approx 6\times10^{17}(0.05/e_{\rm cross})^p \text{ years} \quad (17)$$

(*10*), where p is the exponent of $e_{\rm U}$ in Eq. 8. This estimate is uncertain by a large factor, possibly by one or two orders of magnitude, but it is clear that Uranus will be with us for a long time. The resonance closest to the actual value of $a_{\rm U}$ has $p = 0$.

The discovery that the great inequality was due to the 2:5 near resonance between Jupiter and Saturn clearly had a strong affect on Laplace's views regarding determinism. We find it ironic that the 2:5 resonance plays such a strong role in producing chaos among the outer planets, thereby placing a limit on our ability to state the positions of the jovian planets in the distant future. The fact that Laplace was the first astronomer to identify a three-body resonance in the solar system, involving three of the Galilean satellites, only heightens the irony. More recently, three-body resonances were shown to be responsible for much of the chaos seen in integrations of asteroids (*11*).

Numerical Integrations

To test our theory, we have integrated the equations of motion for the four jovian planets using a symplectic integrator (*12*). We chose this simplified model rather than including all nine planets in order to isolate the effects of the giant planets. To account in a crude way for the effects of the terrestrial planets, we enhanced the mass of the sun by their mass. This ensures that the location of resonances between the jovian planets is shifted by an amount that is second order in this mass ratio, roughly 3×10^{-11}. This is much smaller than the uncertainty in the orbital elements of the planets. The orbital elements, which provide the initial conditions for our integrations, are known to a relative accuracy of a few parts in 10 million. For example, $\Delta a/a \approx 2 \times 10^{-7}$ (600 km for Uranus) (*13*), much smaller than the size of the resonances.

To determine whether the evolution was chaotic, we measured the Lyapunov time by comparing pairs of integrations in which the initial conditions differed by 1.5 mm in the x coordinate of Uranus. Using the DE200 ephemeris from JPL, we confirm the result of Sussman and Wisdom (*3*) that the four jovian planets are chaotic. We find a Lyapunov time of $\sim 7 \times 10^6$ years, consistent with our analytic result and with Sussman and Wisdom's result of $\sim 5 \times 10^6$ years, given that it is difficult to measure Lyapunov times with an accuracy much better than a factor of 2.

To check the robustness of this conclusion, we have carried out integrations in which we varied the initial $a_{\rm U}$ in 10 steps of 300 km; the largest displacement was ± 1500 km, about twice the uncertainty in the JPL ephemeris. We used symplectic correctors (*14*) to ensure that the relative energy errors were less than 10^{-9}, much smaller than the uncertainties in the initial conditions. In all these integrations, we found that the orbits were chaotic.

To test the prediction that the motion is marginally chaotic, we carried out various surveys of the dynamics of the jovian planets in which all the initial orbital elements except $a_{\rm U}$ were held fixed (*15*). The integration time in each survey was 2×10^8 years. In our first survey, we varied the initial value of $a_{\rm U}$ in steps of 0.01 AU between 18.9789 and 19.3990 AU. We found that between 19.18 and 19.399 AU, more than 80% of the orbits are regular. We later conducted a survey in which $a_{\rm U}$ was varied in steps of 0.0001 AU between 19.2141 and 19.2209 AU. The resulting Lyapunov times are plotted as a function of the initial semimajor axis $a_{\rm U}$ in Fig. 1.

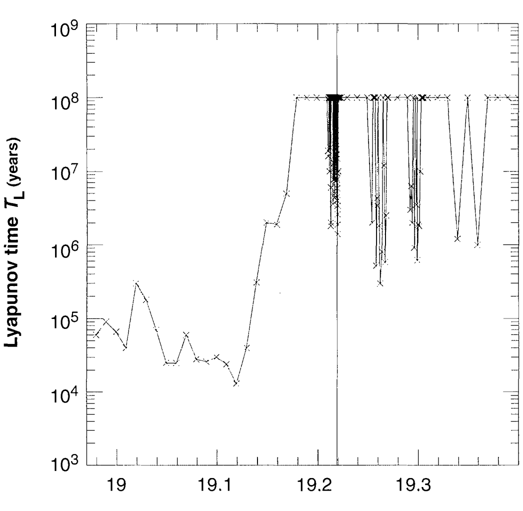

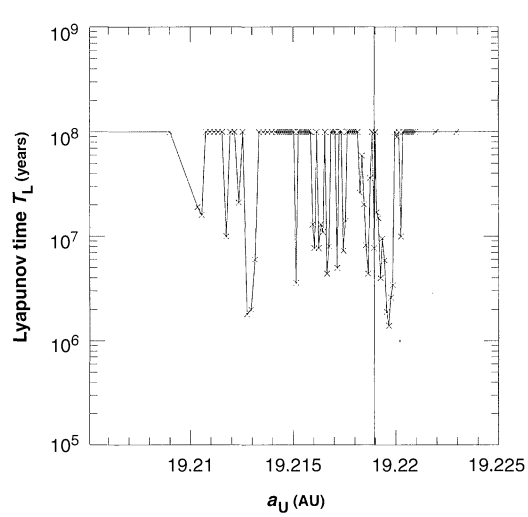

Fig. 1 (left). The Lyapunov time $T_{\rm L}$ as a function of initial $a_{\rm U}$. The initial orbital elements of the planets are taken from DE200, except for $a_{\rm U}$, which is varied. There are chaotic two-body resonances at $a_{\rm U} \approx$ 19.00 and 19.12 AU involving Neptune and Jupiter, respectively. There are also chaotic regions associated with three-body mean motion resonances at $a_{\rm U} \approx$ 19.22, 19.26, 19.29, and 19.34 AU. These involve either Jupiter, Saturn, and Uranus, or Saturn, Uranus, and Neptune. The solid vertical line shows the actual location of Uranus. **Fig. 2 (right).** A close-up of Fig. 1 around the actual value of $a_{\rm U}$. Between 19.216 and 19.218 AU we find the individual eccentricity resonances associated with the resonant argument $3\lambda_{\rm J} - 5\lambda_{\rm S} - 7\lambda_{\rm U} + qg_5 + 7g_6t + (2-q)g_7t$, which do not quite overlap. The resonances associated with the argument $3\lambda_{\rm J} - 5\lambda_{\rm S} - 7\lambda_{\rm U} + qg_5 + 6g_6t + (3-q)g_7t$ lie between 19.218 and 19.221 AU.

We plotted a point at 10^8 years, corresponding to the integration time, if the orbit appeared to be regular. The location of our solar system as represented in the DE200 ephemeris is indicated by the vertical line in the figure. From 18.9789 to 19.15 AU we find a strongly chaotic region, with Lyapunov times ranging from 2.5×10^4 to 2×10^6 years. Examination of the resonant argument $\lambda_U - 2\lambda_N + \omega_N$ reveals that from 18.9789 to ~19.13 AU our pseudo-Uranus is in a 1:2 mean motion resonance with Neptune. From 19.13 to 19.17 AU pseudo-Uranus is in the 7:1 mean motion resonance with Jupiter described by Eq. 7, with a Lyapunov time ranging upwards from 10^5 years. Four other chaotic regions are visible in Fig. 1, centered at $a_U = 19.219$, 19.26, 19.29, and 19.34 AU. All of these regions are associated with three-body resonances.

The dynamics in the region from 19.21 to 19.225 AU (Fig. 2) is controlled by the $3\lambda_J - 5\lambda_S - 7\lambda_U$ three-body resonance described in Eq. 8. We can see the effects of the individual resonant terms. For $a_U < 19.218$ AU the resonances are isolated by regular regions, indicating that the resonance widths are slightly smaller than the distance between resonances. For $a_U \gtrsim 19.218$ AU nearly all the orbits have finite Lyapunov times, indicating that the individual resonances overlap completely. Figure 3 shows the resonant angle $3\lambda_J - 5\lambda_S - 7\lambda_U + 3g_5t + 6g_6t$ (the $q = 0$ case of Eq. 11) for $a_U = 19.21908$, about one planetary radius larger than the value of a_U used in the DE200 ephemeris. It alternates between libration, with a period of $\sim 2 \times 10^7$ years, and rotation, indicating that the orbit is crossing the separatrix of the resonance and confirming the chaotic nature of the orbit. In addition to the $3\lambda_J - 5\lambda_S - 7\lambda_U$ resonance, there is a resonant term involving Saturn, Uranus, and Neptune. Our calculations suggest that this resonance is responsible for the chaotic zones at 19.29 and 19.34 AU, and plays a strong role in the chaotic zone at 19.26 AU.

Integrations of simpler models. In another survey, we set $i = 0$ for all four jovian planets and again varied a_U in steps of 0.01 between 18.9789 and 19.3990 AU, and in steps of 0.0001 between 19.2141 and 19.2209 AU. The general appearance is similar to that of Fig. 1, showing that inclination resonances are not essential to produce chaos among the jovian planets. However, the chaotic region near $a_U = 19.219$ AU is not quite so extensive, and the resonances appear to be isolated, like those with $a_U < 19.218$ AU in Fig. 2. In yet another survey, we removed Neptune. The chaotic region at $a_U \approx 19.00$ AU vanishes, but the chaos associated with $7\lambda_U - \lambda_J$ remains. Similarly, the chaos at $a_U = 19.29$ AU and 19.34 AU is no longer present. However, a chaotic region at $a_U = 19.219$ AU and a very small chaotic region at 19.25 AU remain. The feature near $a_U = 19.219$ AU is even less extensive than in the planar case, indicating that the effects of the $3\lambda_S - 5\lambda_U - 7\lambda_N$ resonance are more important than the effects of inclination resonances involving Jupiter. Finally, a survey in which Neptune is removed and the remaining jovian planets orbit in the same plane reveals no chaotic motion outside the $7\lambda_U - \lambda_J$ resonance. Apparently, eccentricity resonances involving only the inner three jovian planets do not quite overlap. They must act in concert either with inclination resonances or with three-body resonances involving Neptune to produce detectable chaotic regions.

The Epoch of Resonance Capture

Uranus probably did not form in the current resonance. Planet formation is believed to occur in disks around young stars. Evidence for such disks, which have lifetimes around 10^7 years, is now abundant, including visible, infrared, and millimeter observations of disks around young stars (*16*). The observations show that the disks contain both gas and particulate matter. The existence of our own asteroid and Kuiper belts, as well as of comets, suggests that protostellar disks contain larger bodies as well. Current understanding of the planet formation process suggests that planets migrate over substantial distances early in the history of a planetary system. Goldreich and Tremaine (*17*) showed that torques produced by interactions between a gas disk and a planet can cause large-scale planet migrations on time scales of tens to hundreds of thousands of years. Interactions between asteroids or comets and planets can also cause planet migrations (*18*). The recent discovery (*19*) of Jupiter-mass objects in short-period (4 day) orbits around nearby stars strongly suggests that planet migration is common.

We can compare the torques exerted on Uranus by the different processes. Jupiter and Saturn currently exert a resonant torque on Uranus given by

$$T_{\rm res} \approx 100(GM_\odot M_U/a_U)\mu_J\mu_S e_J^{5-p} e_U^p e_S^2/\varepsilon_{JS} \quad (18)$$

The torque exerted on proto-Uranus by the gas disk in which it formed is

$$T_{\rm gas} \approx 5.6(GM_\odot M_U/a_U)\mu_U\mu_g m_{\rm max}^3 \quad (19)$$

(*17*). In this expression the quantity $m_{\rm max}$ is a measure of the gap in the gas disk produced by Uranus. If no such gap formed, the torque produced by the gas disk is even larger. The minimum mass of the solar nebula is ~10 Jupiter masses, so $\mu_g \equiv M_{\rm gas\ disk}/M_\odot \approx 0.01$. The torque produced by interactions between Uranus and a planetesimal disk is

$$T_{\rm planetesimal} \approx (GM_\odot M_U/a_U)(M_d/M_U)(T_U/T_{\rm clear}) \quad (20)$$

where M_d is the total mass of the planetesimals that interact with Uranus, $T_U \approx 80$ years is the orbital period of Uranus, and $T_{\rm clear} \approx 10^7$ years is the time for Uranus to clear the planetesimal disk. In units of $GM_\odot M_U/a_U$ the torques are $T_{\rm res} \approx 10^{-11}$, $T_{\rm gas} \approx 10^{-3}$, and $T_{\rm planetesimal} \approx 10^{-6} M_d/M_U$. The planets remain in resonance only if $T_{\rm res} \gtrsim T_{\rm gas}$ and $T_{\rm res} \gtrsim T_{\rm planetesimal}$. Clearly, Uranus must have been trapped in the resonance after the gas disk dissipated. Similarly, most of the planetesimal disk must be removed before the final trapping can occur.

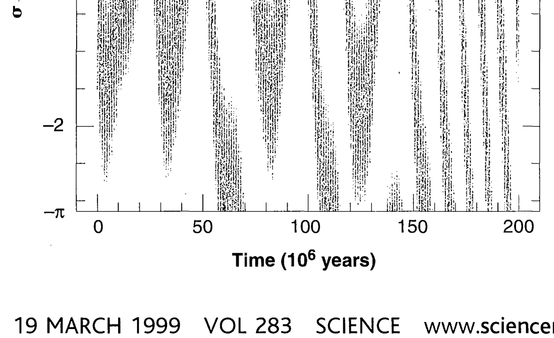

Fig. 3. The resonant argument $3\lambda_J - 5\lambda_S - 7\lambda_U + 3g_5t + 6g_6t$ in the case $a_U = 19.21908$, about one planetary radius larger than the actual value of a_U. The libration period is $T_0 \approx 2 \times 10^7$ years. A transition from libration to rotation occurs near 6×10^7 years. A longer-lasting transition from libration to rotation occurs at 1.6×10^8 years. The Lyapunov time was measured to be $\sim 7 \times 10^6$ years.

References and Notes

1. P. S. Laplace, *Traite de Mecanique Celeste* (Paris, 1799–1825).
2. V. I. Arnold, *Russ. Math. Surv.* **18**, 85 (1961).
3. G. J. Sussman and J. Wisdom, *Science* **241**, 433 (1988); *ibid.* **257**, 56 (1992).
4. J. Laskar, *Nature* **338**, 237 (1989).
5. The orbits have sizes and shapes described by semimajor axis *a* and eccentricity *e*. The orientation of an orbit is described by the inclination *i*, the longitude of the ascending node Ω, and the longitude of perihelion ω, whereas the location of the planet in the orbit

is described by the mean anomaly l or equivalently the mean longitude $\lambda \equiv l + \omega$. Collectively these variables are called orbital elements. In the Kepler problem, where a single planet orbits a spherical star, all the elements of the planet except the mean longitude are fixed, which is why the elements are useful quantities. We use the masses and a, e, and i from the JPL ephemeris DE200 (Table 2).

6. B. V. Chirikov, *Phys. Rep.* **52**, 263 (1979); A. J. Lichtenberg and M. A. Lieberman, *Regular and Chaotic Dynamics* (Springer-Verlag, New York, 1992).
7. M. Holman and N. Murray, *Astron. J.* **112**, 1278 (1996).
8. B. Peirce, *ibid.* **1**, 1 (1849); U.-J. Le Verrier, *Annales de L'Observ. Imp. de Paris* **1**, 1 (1855); a modern computer algebraic expansion to eighth order is given by C. D. Murray and D. Harper, *Expansion of the Planetary Disturbing Function to Eighth Order in the Individual Orbital Elements* (QMW Maths Notes, School of Mathematical Sciences, London, 1993).
9. F. Moulton, *An Introduction to Celestial Mechanics* (Dover, New York, 1970), p. 361.
10. N. Murray and M. Holman, *Astron. J.* **114**, 1246 (1997).
11. ———, M. Potter, *ibid.* **116**, 2583 (1998); A. Morbidelli and D. Nesvorney, *ibid.*, p. 3029; for example, our integrations of asteroid 7690 Sackler show that it is in a three-body resonance involving the asteroid, Jupiter, and Saturn.
12. J. Wisdom and M. Holman, *Astron. J.* **102**, 1528 (1991).
13. M. Standish, personal communication.
14. J. Wisdom, M. Holman, J. Touma, *Fields Inst. Commun.* **10**, 217 (1996).
15. A similar survey is reported by G. D. Quinlan, in *IAU Symposium 152* (Kluwer, Dordrecht, Netherlands, 1992).
16. See, for example, S. V. W. Beckwith, A. Sargent, R. S. Chini, R. Guesten, *Astron. J.* **99**, 924 (1990); K. R. Stapelfeldt *et al.*, *Astrophys. J.* **502**, L65 (1998); A. Dutrey *et al.*, *Astron. Astrophys.* **338**, L63 (1998).
17. P. Goldreich and S. Tremaine, *Astrophys. J.* **241**, 425 (1980).
18. J. A. Fernandez and W.-H. Ip, *Icarus* **58**, 109 (1984); R. Malhotra, *Nature* **365**, 819 (1993); *Astron. J.* **110**, 420 (1995); N. Murray, B. Hansen, M. Holman, S. Tremaine, *Science* **279**, 69 (1998).
19. M. Mayor and D. Queloz, *Nature* **378**, 355 (1995); D. W. Latham, R. P. Stefanik, T. Mazeh, M. Mayor, G. Burki, *ibid.* **339**, 38 (1989); G. W. Marcy and R. P. Butler, *Astrophys. J.* **464**, L147 (1996); R. P. Butler, G. W. Marcy, E. Williams, H. Hauser, P. Shirts, *ibid.* **474**, L115 (1997); R. W. Noyes *et al.*, *ibid.* **483**, L111 (1997); *ibid.* **487**, L195 (1997).

20. We thank B. Gladman and J. Wisdom for helpful conversations. Supported by NSERC of Canada.

28 September 1998; accepted 8 February 1999

Compositional Stratification in the Deep Mantle

Louise H. Kellogg,[1*] Bradford H. Hager,[2] Rob D. van der Hilst[2]

A boundary between compositionally distinct regions at a depth of about 1600 kilometers may explain the seismological observations pertaining to Earth's lower mantle, produce the isotopic signatures of mid-ocean ridge basalts and oceanic island basalts, and reconcile the discrepancy between the observed heat flux and the heat production of the mid-ocean ridge basalt source region. Numerical models of thermochemical convection imply that a layer of material that is intrinsically about 4 percent more dense than the overlying mantle is dynamically stable. Because the deep layer is hot, its net density is only slightly greater than adiabatic and its surface develops substantial topography.

Several fundamental constraints must be satisfied by a successful model of the dynamics and thermochemical structure of Earth's mantle. The model must produce sufficient heat, either by radioactive decay or by cooling of the planet, to account for the inferred global heat flux. The model must be capable of producing the rich variety and the observed systematics of geochemical signatures in mantle-derived basalts (*1*). The model must be consistent with inferences from seismic tomography that some subducted slabs extend to near the base of the mantle (*2*) and that the lowermost mantle is characterized by long wavelength structure (*3, 4*) and complex relations between the bulk sound and shear wavespeed (*5, 6*) [see (*7*) for an overview]. Finally, the model must be dynamically consistent. Here, we present a model that is dynamically feasible and satisfies the essential geochemical and geophysical observations. It differs from many previous models by placing a boundary between compositionally distinct mantle regions deep in the lower mantle, rather than at a depth of 660 km.

The characteristic isotopic ratios of mid-ocean ridge basalts (MORB) and oceanic island basalts (OIB) provide evidence for a suite of distinct reservoirs in the mantle (*1*). These reservoirs and signatures are thought to be produced by the formation and recycling of oceanic crust and lithosphere, plus small amounts of recycled continental crust. In addition, ^{129}Xe, ^{3}He/^{4}He, and ^{40}Ar contents of the mantle (*8–10*) indicate that the mantle has not been entirely outgassed.

^{87}Sr/^{86}Sr and ^{143}Nd/^{144}Nd isotope ratios of the crust and MORB have been used to estimate the mass of mantle from which the crust was extracted, and hence to infer the mass of the remaining, less depleted component. Estimates for the mass of the depleted mantle range from 25% (*11*) (coincidentally the mass of the mantle above the 660-km discontinuity) to 90% (*1*). Similar mass balance arguments are used to determine the amount of mantle that must have been outgassed to produce the ^{40}Ar in Earth's atmosphere (*10*); these predict a volume of degassed mantle of ~50%. Uncertainties arise because the K/U ratio of Earth is still under debate (*12*) and the lower crust or the undegassed parts of the mantle have retained substantial amounts of ^{40}Ar (*13*), or some Ar may be recycled.

Another fundamental constraint is provided by Earth's heat budget (*14, 15*). Of the 44 TW (*16*) of the present-day heat flux out of Earth, 6 TW is generated within the crust by radioactive decay of U, Th, and K, and 38 TW must be provided either by generation of heat within the mantle and core or by cooling of the planet (*17*). For example, if Earth had the radiogenic heat production of the average chondritic meteorite, the total heat production would be 31 TW; the remaining 13 TW would be provided by cooling of the planet by 65 K per 10^9 years. Geochemical analyses of basalts, however, show that the source region of MORBs is depleted in heat production by a factor of 5 to 10 relative to a chondritic silicate value (*18*). Thus, if the MORB source region made up most of the mantle, the mantle heat production would be only 2 to 6 TW, comparable to that of the crust. Matching the observed heat flux would require rapid cooling of the planet by, on average, 175 K per 10^9 years, which requires excessive internal temperatures during the Archaean (*19*).

Hence, there must be an extra heat source. The D'' region, a layer of anomalous seismic velocities several hundred kilometers thick at the base of the lower mantle, is likely to be compositionally distinct (*20*), but it can account for only a small fraction of the global heat flux unless there is extreme internal heat production. The latter is unlikely, in particular if the D'' layer contains foundered oceanic crust (*21*), which has a heat production comparable to that of the chondritic silicate Earth (*17*), or some core material (*22*), which is likely low in U, Th, and K.

The energy calculations and geochemical mass balances both suggest that the mantle is composed of several reservoirs: a depleted region, which is the source of MORB; a region that, relative to the MORB source, is unde-

[1]Department of Geology, University of California, Davis, CA 95616, USA. [2]Department of Earth, Atmospheric, and Planetary Sciences, Massachusetts Institute of Technology, Cambridge, MA 01239, USA.

*To whom correspondence should be addressed.